 doi:10.20944/preprints202207.0352.v1

Article

Dynamic Shear Modulus and Damping of MICP-treated Calcareous Sand at Low Strains

Xinlei Zhang [1], Jun Guo [1], Yumin Chen [2,*], Yi Han[2], Ruibo Yi [1], Hongmei Gao [1], Lu Liu [1], Hanlong Liu [3], Zhifu Shen [1]

[1] Research Center of Urban Underground Space, Nanjing Tech University, Nanjing 211816, China. Xinlei Zhang: E-mail: xinlei.zhang@njtech.edu.cn; Jun Guo: E-mail: 201961125012@njtech.edu.cn; Ruibo Yi: E-mail: 202061125014@njtech.edu.cn; Hongmei Gao: E-mail: hongmei54@njtech.edu.cn; Lu Liu: E-mail: lliu@njtech.edu.cn; Zhifu Shen: E-mail: zhifu.shen@njtech.edu.cn.

[2] College of Civil and Transportation Engineering, Key Laboratory of Ministry of Education for Geomechanics and Embankment Engineering, Hohai University, Nanjing 210098, China. Yumin Chen: E-mail: ymch@hhu.edu.cn; Yi Han: 210204030002@hhu.edu.cn.

[3] College of Civil Engineering, Key Laboratory of New Technology for Construction of Cities in Mountain Area, Chongqing University, Chongqing 400045, China. Hanlong Liu: E-mail: 160204010011@hhu.edu.cn.

* Correspondence: ymch@hhu.edu.cn.

Abstract: Calcareous sand deposits are widely distributed along the shoreline in tropical and subtropical regions. Microbially induced calcite precipitation treatment (MICP) is a relatively new method to improve the stiffness and strength of the soil. Little is known about the small-strain shear modulus and damping ratio of MICP-treated calcareous sand, which are two crucial parameters for the prediction of the dynamic behavior of soil. A series of resonant column tests are performed to investigate the dynamic performance of MICP-treated calcareous sand, with special attention paid to the influence of treatment duration and confining stress on the stiffness and damping characteristics. The relationship between the initial dynamic shear modulus and unconfined compressive strength is analyzed. Additionally, the empirical equations of the reference shear strain between treatment duration and confining stress are given. The G/G_0 of MICP-cemented calcareous sand presents a higher strain sensitivity than that of untreated sand, and its attenuation pattern can be described by Hardin-Drnevich model. The σ_c has an apparent effect on the degradation characteristics of the dynamic shear modulus of MICP-treated calcareous sand with a low cementation level, however, its effect decreases with the increasing treatment duration. The relationship between the reference shear strain and the treatment duration and confining stress can be described by a power and a linear formula, respectively.

Keywords: Calcareous sand; Microbially induced calcite precipitation; Dynamic shear modulus; Resonant column test; Reference shear strain

1. Introduction

Calcareous sand is widely distributed along the coastline of the South China Sea, the Red Sea, Australia, the Gulf of Mexico, and other tropical or subtropical regions [1], which is an essential part of construction material in coastal structures. Calcareous sand usually consists of the reworked shell fragments and skeletal debris of marine organisms [2,3]. Calcareous sand has special features, such as irregularly shaped particles, porous interior, polygonal angle, crushable grain, etc. [4]. As a result, the mechanical behavior of calcareous sand can be considerably different from siliceous sands due to their different mineral resources and particle characteristics [5,6].

Several conventional geotechnical applications including grouting, densification and deep mixing have been explored to improve the bearing capacity and liquefaction resistance of siliceous sand [7]. However, these methods may be not suitable for the treatment of artificial calcareous sand islands which are far from the inland and with a poor construction environment. In recent years, microbially induced calcite precipitation

 doi:10.20944/preprints202207.0352.v1

(MICP), a new technology that utilizes biological metabolic processes to improve soil properties has been developed [8-10]. The fundamental chemical reactions governing the MICP process can be simply specified as follows [11,12]:

$$CO(NH_2)_2 + 2H_2O \rightarrow 2NH_4^+ + CO_3^{2-}$$

$$Ca^{2+} + CO_3^{2-} \rightarrow CaCO_3 \downarrow$$

Compared with the conventional soil improvement methods, MICP has many advantages such as being environmentally friendly, further transmission distance, small disturbance, and controllability of the process [13,14]. MICP has been applied to solve practical engineering problems including improved soil strength and stiffness [12,15], reduced soil permeability [16], repaired cracks in the structure [17], and erosion control [18]. Recently, MICP treatment has been proved to be effective to improve the static strength and liquefaction resistance of calcareous sands [1,8,19] due to the calcite crystal precipitated between the sand particles which strengthens the soil structure.

However, the information regarding dynamic aspects of MICP-treated calcareous sand at low strains, such as small-strain dynamic shear modulus and damping ratio, is limited. The dynamic shear modulus and damping ratio are the essential parameters to analyze the dynamic response of soil during dynamic loading conditions, such as earthquakes, traffic loads, and wave loads [20]. Over the past few decades, the dynamic properties of calcareous sand have been widely investigated in the laboratory [20,21]. For example, the small-strain shear modulus and damping ratio of calcareous sand under isotropic or anisotropic stress consolidated state have been studied [22–25]. The effects of confining stress, pore ratio, relative density, grading and particle size, and particle breakage on the dynamic properties are discussed [21,25–29]. Morsy et al. [26] found the effect of void ratio on shear modulus was more pronounced at low void ratios and maximum shear modulus increased as the void ratio decreased. Javdanian and Jafarian [27] performed resonant column and cyclic triaxial test on two marine calcareous sands and found shear stiffness ratio increased and damping ratio decreased with the increase the effective confining pressure. Hassanlourad et al. [28] studied the shear behavior of calcareous sand through drained and undrained triaxial tests and reported the effect of particle breakage on specimen response. Khalil et al. [29] performed a series of bender element and cyclic triaxial tests to study the low-strain and large-strain characterization of calcareous sand and terrigenous sand.

Although, the dynamic shear modulus and damping ratio at low strains have been extensively studied on natural soil and cement stabilized soil [22,26,29–34], considerably less information is available for the dynamic response of marine soil like calcareous sand at different MICP--treatment levels. It is necessary to understand how the shear modulus and damping ratio of MICP-treated calcareous sand varied with shear strain and other factors for engineering application. Numerous studies have shown that the mechanical properties of cemented soils are determined by the cementation level [15,35] and confining stress [36–39]. Accordingly, the main objective of this study is to study the dynamic behavior of MICP-treatment calcareous sands at low strain amplitude, with a focus on the effects of confining stress and treatment time related to the precipitated calcite contents. A series of resonant column tests were conducted to evaluate the dynamic shear modulus and damping ratio of calcareous sandy at a low MICP-treated level. In this paper, first, the test materials and implementation methods are described. Next, the effect of MICP treatment on the dynamic response of saturated calcareous sand at low shear strain is discussed, including the responses of the dynamic shear modulus, degradation characteristic of normalized dynamic shear modulus, and damping ratio. In addition, the correlations of initial dynamic shear modulus with unconfined compression strength, confining stress, and treatment time are discussed and summarized. Finally, empirical relations of reference shear strain and the treatment time, and the confining stress are proposed. The results of this study would provide the quantification of dynamic parameters of MICP-treated calcareous sand and relevant support for the development of constitutive models.

Preprints (www.preprints.org) | NOT PEER-REVIEWED | Posted: 25 July 2022 doi:10.20944/preprints202207.0352.v1

2. Materials and Methods

2.1. Material properties

The calcareous sand used in the current study was obtained from an island in the South China Sea, and its particle size distribution curve is presented in Figure 1. The calcium carbonate content of this sand is more than 90.25%, as obtained from the chemical componential analysis, and its microscope (SEM) images are shown in Figure 2. A summary of the sand parameters is presented in Table 1. The calcareous sands have a coefficient of uniformity of $C_u = 3.55$ and a coefficient of curvature of $C_c = 0.97$, and is classified as poorly graded sand according to the Unified Soil Classification System.

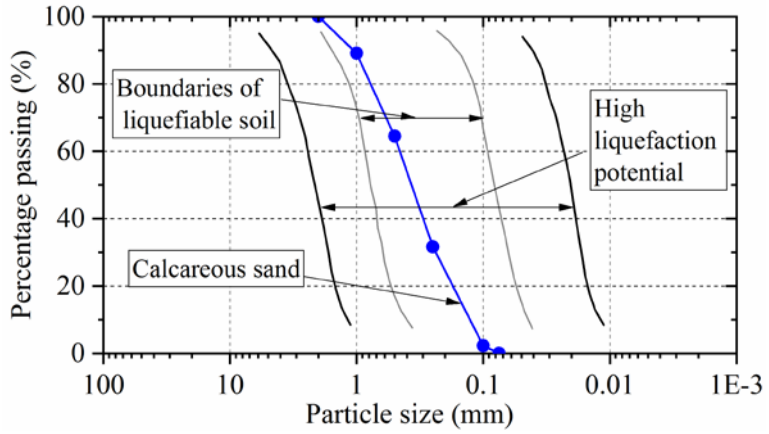

Figure 1. Particle size distribution curve of calcareous sand used in this study.

Figure2. Scanning electron microscope (SEM) images (in different close-up views) of the calcareous sand used in this study.

Table 1. Index properties for the calcareous sand used in this study.

Sand	D_{50} (mm)	D_{10} (mm)	C_u	C_c	G_s	e_{min}	e_{max}	Shape
Calcareous sand	0.38	0.13	3.55	0.97	2.73	1.02	1.44	irregular

2.2. MICP treatment procedure

 doi:10.20944/preprints202207.0352.v1

Sporosarcina pasteurii (American Type Culture Collection, ATCC11859) is an aerobic uratolytic bacterium, which uses urea as a nutrient and produces CO_3^{2-} as the key part of $CaCO_3$ precipitation. The bacterial fluid was cultured in a medium solution (with a ratio of 1:10), whose composition is presented in Table 2. The bacteria were enlarged in an incubator shaker at 30 °C at speed of 210 rpm for approximately 24–32 h. The optical density (OD600) of the harvested bacterial was about 0.71, and the urease activity was approximately 1.1 mM urea hydrolyzed per minute. The cementation solution (CS) used in the experiments was a mixture of 0.5 mol/L urea and 0.5 mol/L $CaCl_2$. The volume of cementation solution used for each sample in the tests is about 7 times the sample pore volume, i.e., 720 mL.

Table 2. Biological media

Reagent	Concentration
Yeast extract	20 g/L
NH_4Cl	10 g/L
$MnCl_2{\cdot}H_2O$	12 mg/L
$NiCl_2{\cdot}6H_2O$	24 mg/L
Distilled water	1000 g/L
1 mol/L NaOH	pH value approximately 9

To achieve batches of intact samples, the calcareous sandy samples were prepared by using a series of specially-designed specimen preparation devices. The procedure for preparing samples is shown in Figure 3. The specimen's preparation device consists of two semi-cylindrical PVC moulds to disassemble the device and get the soil sample out of the mold easily, two pieces of filter fabric to prevent the fine sand particles from being flushed out during the treatment process, a small aspirating hole on the mold to connect with the vacuum pump and two PVC pedestal. The internal diameter and height of the PVC split mold are 5 and 10 cm, respectively. A thin rubber membrane is attached to the inner walls of the columniform mold. During the process of the sample preparation, a vacuum pump is connected with the aspirating hole on the mold to draw a negative pressure between the rubber membrane and the inner wall of the mold without leaving any gaps to achieve standard diameter samples.

The samples of 50 mm diameter and 100 mm high are prepared in the split mold. The sample preparation process could be divided into several steps. Firstly, the dry calcareous sands of about 345g were packed into the thin rubber membrane in five consecutive layers. It should be ensured that each layer was filled evenly and made sure the surface of the last layer was as smooth as possible. The relative density of the reconstituted specimens is controlled at about 40%. Secondly, after the sand sample was prepared, 110 ml of the bacterial liquid was pumped into the sand specimen at a rate of 180 mL/h through the peristaltic pump. After the bacterial solution had been inoculated, it was detained in the soil pore space for a period of at least 6 h to allow the bacteria to diffuse and adhere to the soil particles. Thirdly, after the detention of the bacterial fluid, the cementation solution was pumped into the soil sample at a rate of 180 mL/h and flowed out freely by the pipe on the top cover. Finally, after treatment, all specimens were washed repeatedly with four pore volumes of distilled water to purge them of the bacterial solution and residual cementation solution, and another purpose is to saturate the sample.

Preprints (www.preprints.org) | NOT PEER-REVIEWED | Posted: 25 July 2022 doi:10.20944/preprints202207.0352.v1

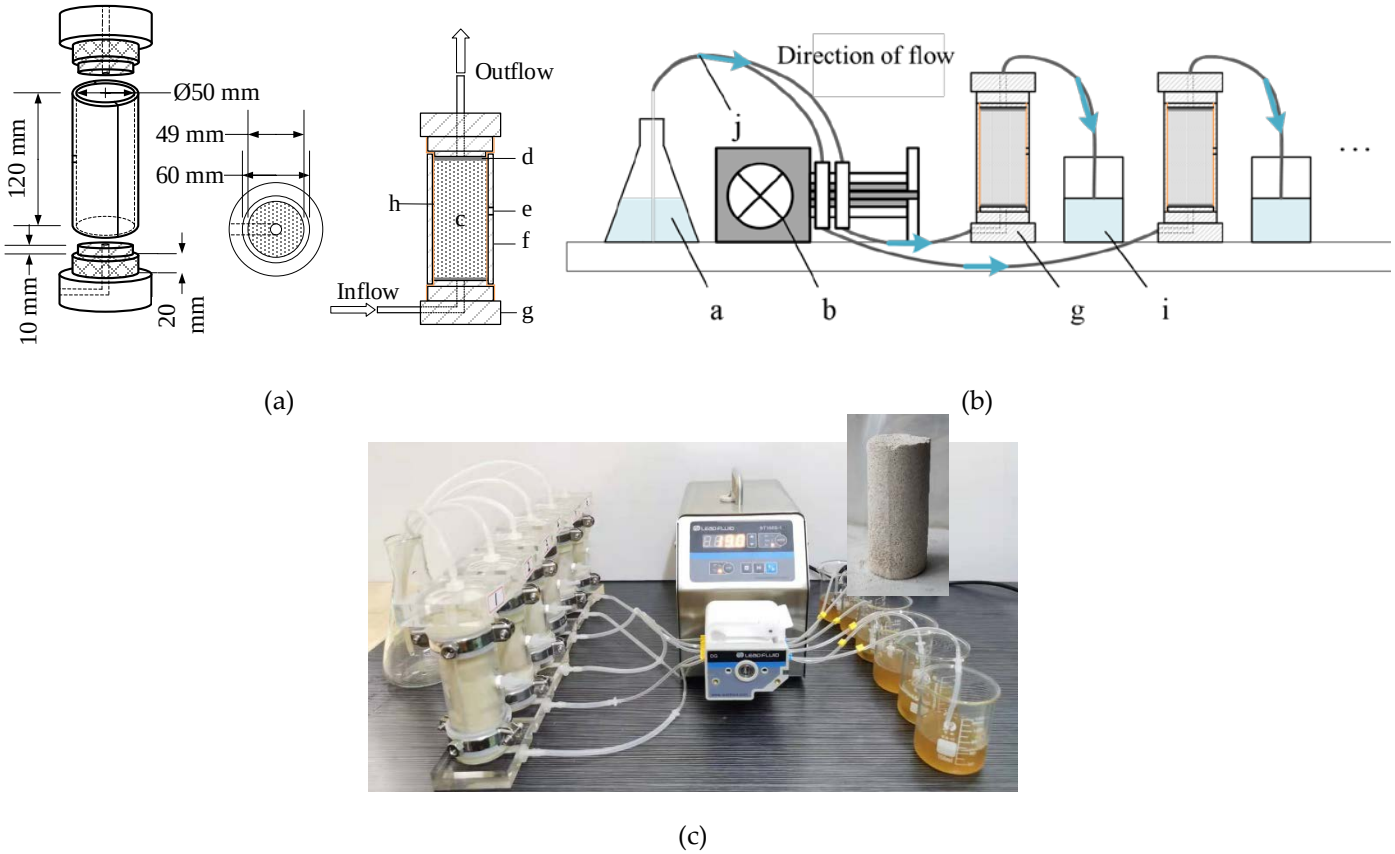

Figure 3. Schematics of MICP treatment device for: (a) Diagrammatic schematics of mould for MICP-treated cylindrical specimens, (b) Schematic of MICP treated calcareous sand, and (c) Sketch of MICP treatment procedure. (a. Bacterial liquid/ cementation solution; b. Peristaltic pump; c. Sand sample; d. Filter fabric; e. Aspirating hole; f. PVC split mold; g. PVC pedestal; h. Rubber membrane; i. Effluent; j. Plastic tube)

2.3. Equipment and testing procedure

The experiments pertaining to the MICP-treated calcareous sand were performed using the resonant column facility developed by GCTS as shown in Figure 4(a). The resonant column apparatus is of bottom-fixed and top-free configuration and can be adjusted according to the size of prepared soil specimens. The air-filled cell of the apparatus can pressure up to 1 MPa and there is an internal high-resolution LVDT for measurement of the deformation of specimens. The back-pressure saturated method was applied to ensure that the specimens were saturated and the applied back-pressure is 400 kPa. The *B*-values of more than 0·95 was achieved in all the specimens in this study. Then, the effective confining stress was applied to the target value and held constant. Shear modulus and damping ratio were calculated by combining the frequency-response curve, specimen size, and parameter of the apparatus. After completing the tests, all sand specimens were oven-dried at 65°C for at least 72h and weighted.

A series of unconfined compressive tests were conducted to analyze the relationship between the static strength and the dynamic properties of MICP-treated calcareous sand. The unconfined compressive strength of MICP-treated samples was measured using a YSH-2 type of unconfined compression apparatus (Figure 4(b)). The upper and lower surfaces of the samples were scraped flat and placed on the unconfined compressive apparatus. The loading speed was set to be 1mm/min, and the unconfined compression strength of the soil samples was measured. The samples were oven-dried to measure the content of $CaCO_3$ after unconfined compressive tests or resonant column tests. The content of $CaCO_3$ could be evaluated based on the following formulation:

Preprints (www.preprints.org) | NOT PEER-REVIEWED | Posted: 25 July 2022 doi:10.20944/preprints202207.0352.v1

$$C_{CaCO_3}(\%) = \frac{m_0 - m}{m} = \frac{\Delta m}{m} \times 100 \quad (1)$$

where C_{CaCO3} is the content of $CaCO_3$ in the specimen; m and m_0 are the mass of dry specimen before and after MICP treatment; Δm is the mass of $CaCO_3$.

(a)

(b)

Figure 4. Experimental equipment used in this study for (a) Resonant column device and (b) Unconfined compression test.

2.4. Experimental program

In this study, a total of eighteen groups of resonance column tests were conducted, including fifteen groups of treated conditions and three groups of the untreated conditions to enable comparison with the treated samples. The effects of treatment times (e.g., 6 h, 12 h, 18 h, 24 h, and 48 h) and effective confining stress (e.g., 25 kPa, 50 kPa, and 100 kPa) were considered. Besides, five groups of unconfined compressive tests were carried out to establish the relations between the initial dynamic shear modulus and unconfined

Preprints (www.preprints.org) | NOT PEER-REVIEWED | Posted: 25 July 2022 doi:10.20944/preprints202207.0352.v1

compressive strength. The details of the samples and the contents of $CaCO_3$ are presented in Table.3.

Table 3. Summary of experiments conducted.

Group	Case	Test	Treatment time (hours)	Effective confining stress σ_c (kPa)	D_r (%)	m (g)	e_0	Δm (g)	C_{CaCO3} (%)
Group UN	UN1	RCT	/	/	41.3	236.4	1.27	/	
	UN2	RCT	/	/	39.2	235.5	1.28	/	
	UN3	RCT	/	/	40.5	236.0	1.27	/	
Group M-A	M11	RCT	6	25	40.1	235.9	1.27	5.28	2.24
	M12	RCT	6	50	38.6	235.2	1.28	5.02	2.13
	M13	RCT	6	100	42.3	236.8	1.26	4.98	2.10
	M21	RCT	12	25	39.5	235.6	1.27	8.56	3.63
	M22	RCT	12	50	40.9	236.2	1.27	8.67	3.67
	M23	RCT	12	100	41.1	236.3	1.27	8.21	3.47
	M31	RCT	18	25	39.5	235.6	1.27	11.42	4.85
	M32	RCT	18	50	39.9	235.8	1.27	12.61	5.35
	M33	RCT	18	100	40.2	235.9	1.27	11.89	5.04
	M41	RCT	24	25	41.8	236.6	1.26	17.67	7.47
	M42	RCT	24	50	39.8	235.7	1.27	16.93	7.18
	M43	RCT	24	100	40.8	236.2	1.27	17.24	7.30
	M51	RCT	48	25	40.2	235.9	1.27	25.24	10.70
	M52	RCT	48	50	37.9	234.9	1.28	26.96	11.48
	M53	RCT	48	100	39.4	235.5	1.27	26.68	11.33
Group M-B	M1	UCT	6	/	42.1	236.7	1.26	5.98	2.53
	M2	UCT	12	/	40.8	236.2	1.27	8.65	3.66
	M3	UCT	18	/	42.5	236.9	1.26	13.54	5.72
	M4	UCT	24	/	41.1	236.3	1.27	17.65	7.47
	M5	UCT	48	/	39.5	235.6	1.27	27.16	11.53

Note: UN means an untreated condition, M means MICP-treated condition; RCT means resonant column test, UCT means unconfined compressive test

3. Tests Results and Discussion

3.1. Dynamic shear modulus of MICP-treated calcareous sands

The major nonlinearity in stress-strain behavior of soil is presented by two parameters of the shear modulus G and damping ratio D, which change with shear strain amplitude. Figure 5(a) shows the variation of G with the shear strain γ ranging from 10^{-4} to 4×10^{-2} %. The corresponding shear modulus of the clean sands used in this investigation ranged from 58 to 20 MPa, 63 to 23 MPa, and 95 to 50 MPa at confining stress of 25, 50, and 100 kPa, respectively.

At low confining stress of 25 kPa, the dynamic shear modulus of the soil after treatment is not significantly increased when the treatment duration is less than 18 hours. It is because the amount of precipitated calcium carbonate in the specimens with a low treated

Preprints (www.preprints.org) | NOT PEER-REVIEWED | Posted: 25 July 2022 doi:10.20944/preprints202207.0352.v1

level is limited and the stiffness of these cementations is low, indicating a higher $CaCO_3$ content is required for the loose and porous calcareous sands to form an effective bonding network. In general, under the same loading conditions, the treated sands present a higher shear modulus than that of the untreated sands at the small shear strain.

As the shear strain increases, the shear modulus of the MICP-treated sand decreases gradually and eventually approaches that of the untreated calcareous sand when the shear strain is approximately 0.03%. This observation indicated that the beneficial effect of calcite bonding between sand particles induced by MICP treatment is disappeared when the shear strain exceeds 0.03%. Similar results had been found in the research on cemented sand by Simatupang et al. [36]. For lower confining stress and shorter treatment duration condition, the shear strain level, where the shear modulus of the MICP-treated sand decreases to the untreated value, is generally lower.

Figure 5(b) shows the dynamic shear modulus under different confining stress. The difference in the behavior of shear modulus between treated sand and untreated sand becomes more obvious as the increases of confining stress. This is because the amount of effective contact between sand particles and/or calcium carbonate precipitation is affected by the confining stress, which would certainly change the dynamic shear modulus.

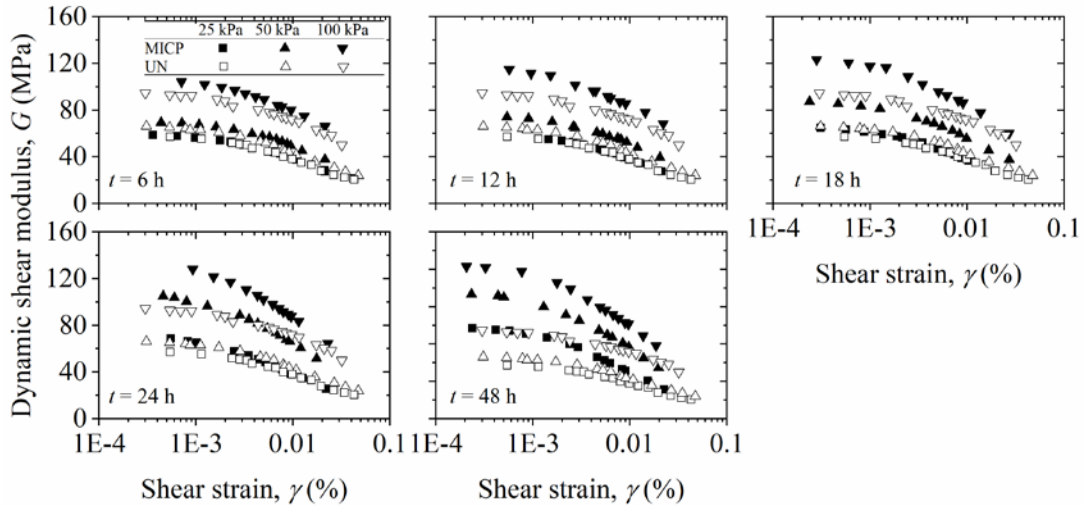

(a)

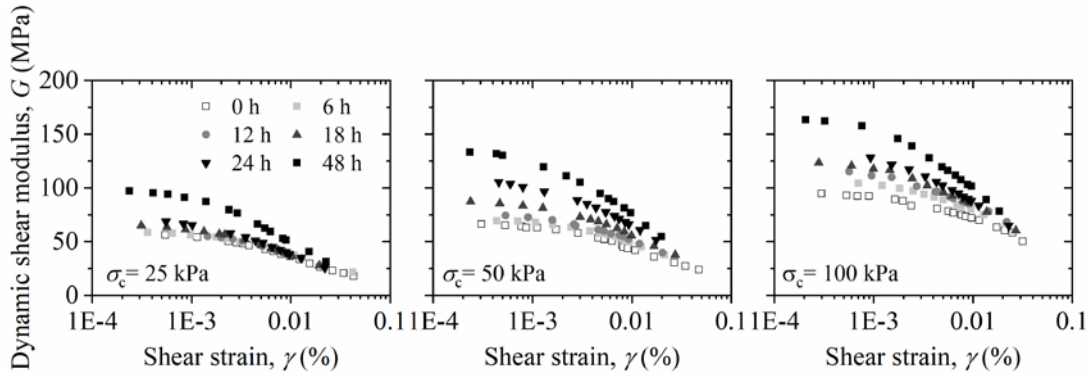

(b)

Figure 5. Dynamic shear modulus attenuation curves of calcareous sand and MICP treated calcareous sand under (a) different treatment time and (b) different confining stress.

3.2. Initial Shear Modulus, G_0

The initial shear modulus, G_0, is a fundamental material property and critical for the dynamic analysis of soils or other materials and defined as the shear modulus at a small strain amplitude of 10^{-4}%.

Preprints (www.preprints.org) | NOT PEER-REVIEWED | Posted: 25 July 2022 doi:10.20944/preprints202207.0352.v1

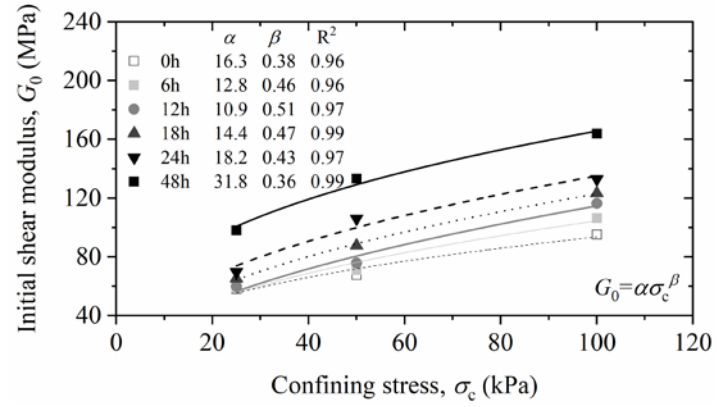

(a)

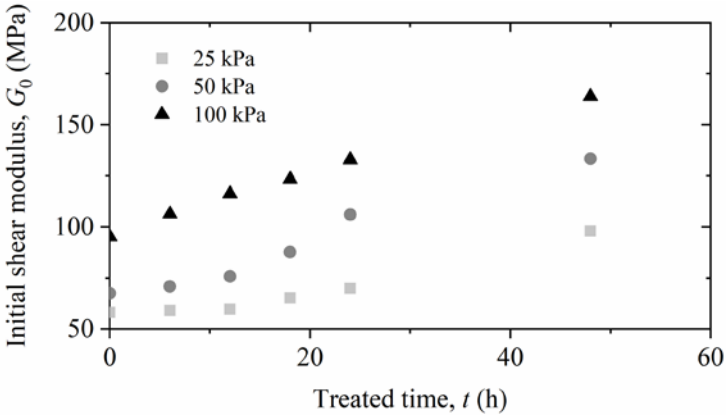

(b)

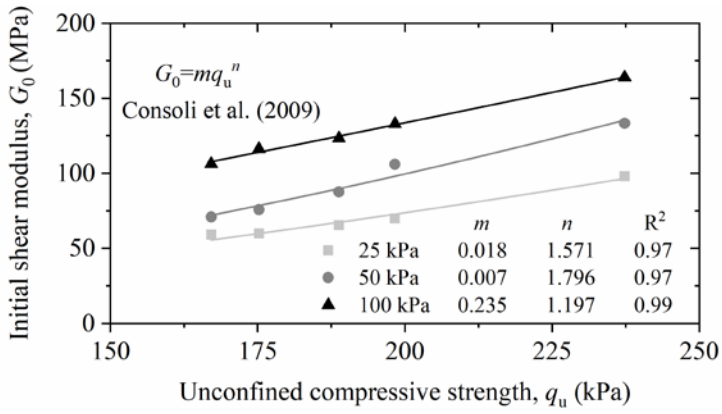

(b)

Figure 6. Initial shear modulus versus (a) confining stress, (b) treatment time, and (c) unconfined compressive strength.

Figure 6(a) shows the effect of confining stress on the initial shear modulus. The initial shear modulus increased with the confining stress and the relationship between them can be satisfactorily expressed by a power function of Eq. (2). proposed by Hardin et al [41].

$$G_0=\alpha\cdot\sigma_c^{\beta} \quad (2)$$

where G_0 is the initial shear modulus; α and β are the fitting parameters related to cement level, void ratio, and other factors; σ_c is the confining stress. R-square is an index to describe the prediction function that fits the real data points. The R-square is greater than

 doi:10.20944/preprints202207.0352.v1

0.96 in all cases. As the treatment time increased from 12 hours to 48 hours, the α increased from 10.9 to 31.8 and the β decreased from 0.51 to 0.36.

Figure 6(b) shows the relationship between the initial shear modulus and the treatment time. It is conspicuous that the increasing treatment time contributed to the increase of G_0 which is attributed to the calcite cementation gradually precipitating with the increasing time. The shear modulus of untreated sands at confining stress of 25 kPa, 50 kPa, and 100 kPa is 58 MPa, 68 MPa, and 95 MPa, respectively, while it is about 98 MPa, 133 MPa, and 164 MPa after treated 48 hours.

When the MICP-treated time is less than 18 hours, the difference in the dynamic shear modulus of the treated samples under low confining stress (25 kPa and 50 kPa) is not obvious compared with the untreated conditions. However, under the confining stress of 100 kPa, the dynamic shear modulus of the treated samples is much higher than that of the untreated samples. This is mainly because the calcareous sands used in the tests are loose and porous, and the calcium carbonate precipitated in the pores is difficult to form effective contacts in the cases with short treatment time. Therefore, the dynamic shear modulus in MICP-treated calcareous sands is not significantly improved at lower confining stress (such as 25 kPa and 50 kPa). The neighboring particles get clustering under higher confining pressure, and the calcium carbonate particles precipitated in the pores which do not contributed to the shear strength have the potential to become effective contact points, which improves the initial dynamic shear modulus of the samples.

The initial shear modulus G_0 and the unconfined compressive strength q_{ucs} are representing two of the most important parameters for soil stiffness and strength [37]. Researchers have found that it is possible to generate a reliable correlation between the G_0 and q_{ucs} for the cemented soil [42,43]. Furthermore, compared with the resonant column test, the unconfined compression strength test is simpler and more efficient, and it is widely applied in civil engineering. In this study, the average peak stress obtained from two replicate specimens was used as the representative unconfined compressive strength. The variation of G_0 with q_{ucs} for bio-treated samples under different confining stress is shown in Figure 6 (c). The G_0 increased with the q_{ucs}, and the relationship between them can be expressed by a power function presented by Consoli et al. [42]:

$$G_0 = m \times q_{ucs}^{n} \tag{3}$$

where G_0 is expressed in MPa, q_{ucs} is expressed in kPa, constants m and n are the fitting parameters in the formula. The *R-square* is greater than 0.98 in all cases. G_0 of treated sands increases non-linearly with an increase of q_{ucs}, which is a direct function of the calcite content precipitated in the specimens.

3.3. Degradation characteristics of normalized dynamic shear modulus

The degradation characteristics of strain-dependent normalized dynamic shear modulus (G/G_0) are important to predict and describe the non-linear dynamic response of soil. Figure 7 shows the normalized shear modulus degradation curves of the MICP-treated sands at low strains. As shown in Figure 7 (a), the degradation of G/G_0 with γ in the higher confining stress is much slower under the same treatment time.

After MICP treatment, the G/G_0 of the calcareous sandy sample decreases quickly with the increasing strain due to the gradual degradation of the bonding between sand particles. It means that the non-linear dynamic characteristic of MICP-treated calcareous sand is more obvious, which is also reported in other types of treated soil [36,37,40,44]. In addition, the strain sensitivity demonstrates more obvious for the samples with a longer treatment time, which indicates that the brittleness of MICP-treated calcareous sands is increased during the treatment process.

The Hardin-Drnevich model [45] (Eq. (4)) has been widely applied to describe the nonlinear relationship between the G/G_0 and γ. This model allows the behavior of the normalized shear modulus reduction to be expressed by two parameters.

Preprints (www.preprints.org) | NOT PEER-REVIEWED | Posted: 25 July 2022 doi:10.20944/preprints202207.0352.v1

$$G/G_0 = 1/(1+(\gamma/\gamma_r)^{\zeta}) \quad (4)$$

where γ_r is the reference shear strain, which is defined as the shear strain corresponding to $G/G_0 = 0.5$, and ζ is the curvature coefficient used to control the curvature of the normalized modulus attenuation curve.

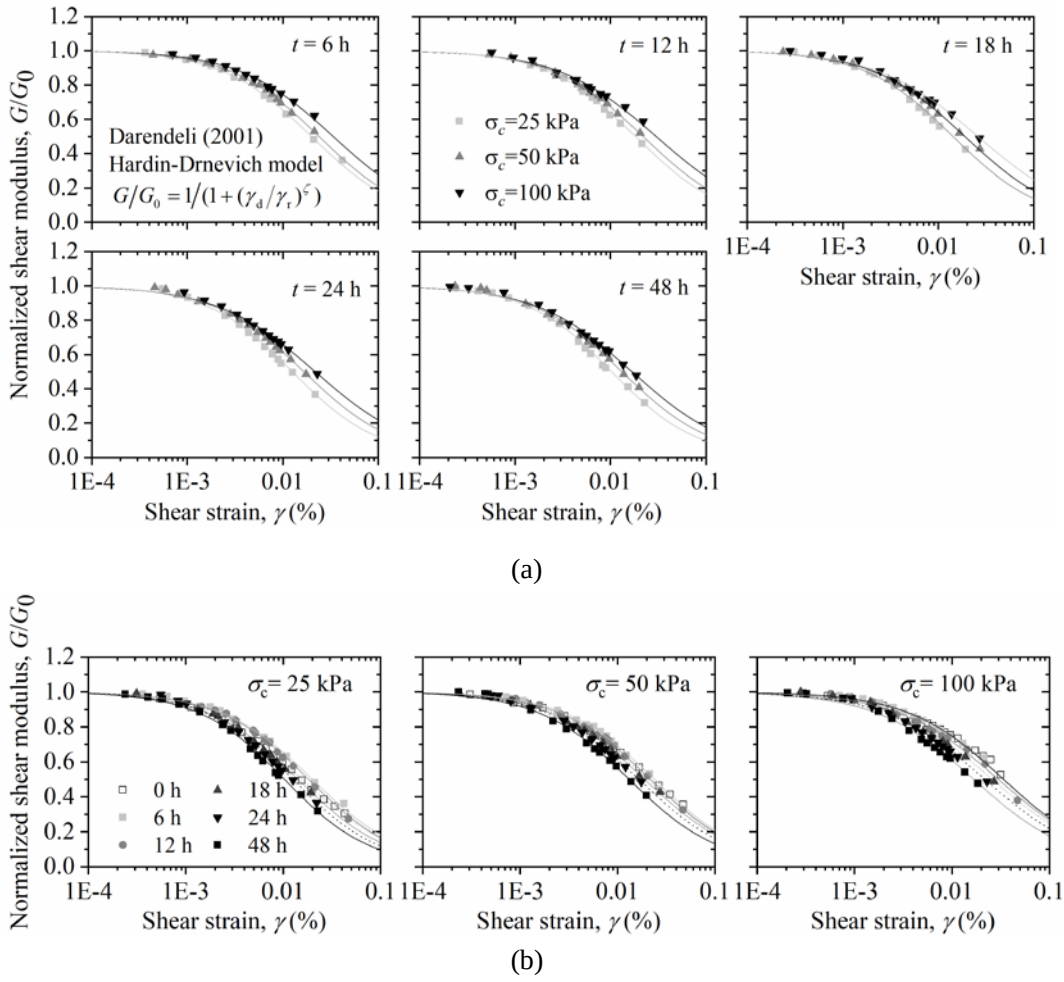

Figure 7. Effect of (a) confined pressure and (b) treatment time on normalized shear modulus.

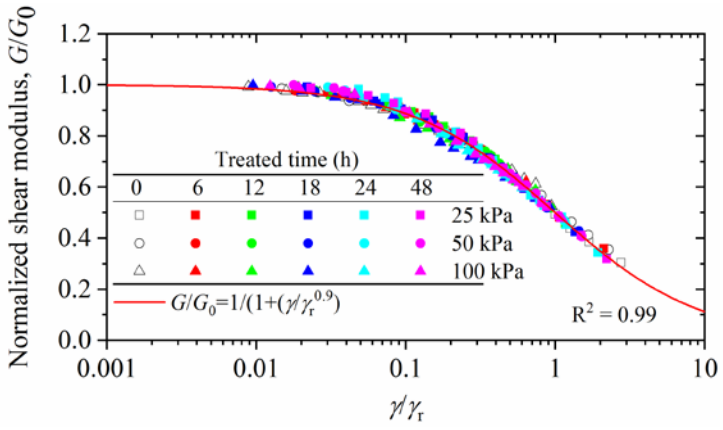

Figure 8. Relationship between normalized dynamic shear modulus and lnγ/γ_r

All the experiments in this study show that the G/G_0-lnγ curves of MICP-treated calcareous sands could be well fitted using the Hardin-Drnevich model, *R-square* is greater than 0.98 in all cases. The parameters of the Hardin-Drnevich model are summarized in

Preprints (www.preprints.org) | NOT PEER-REVIEWED | Posted: 25 July 2022 doi:10.20944/preprints202207.0352.v1

Table 4. The value of ζ which is controlling the curvature of the dynamic shear modulus attenuation curve ranges from 0.83 to 0.99, and it decreases with the increase of confining stress. For lower confining stress and shorter treatment duration condition, the reference shear strain is generally lower.

While the shear strain γ is divided by the reference shear strain γ_r, a best-fit hyperbolic curve for all the data points (G/G_0- ln γ/γ_r) is shown in Figure 8. The fitting parameter ζ is 0.9. The *R-square* is 0.99, which indicates that the model can be used to describe the behavior of stiffness attenuation in both treated and untreated calcareous sand. Therefore, the degradation characteristics of normalized dynamic shear modulus can be satisfactorily represented by only one parameter, that is, γ_r.

Table 3. Summary of experiments conducted.

Treatment time, t(h)	Confining stress, σ_c								
	25kPa			50kPa			100kPa		
	ζ	γ_r/%	R^2	ζ	γ_r/%	R^2	ζ	γ_r/%	R^2
6	0.93	0.01989	0.997	0.93	0.02389	0.997	0.88	0.03362	0.991
12	0.95	0.01844	0.997	0.92	0.02186	0.996	0.84	0.02990	0.984
18	0.94	0.01423	0.996	0.90	0.01893	0.998	0.83	0.02590	0.998
24	0.97	0.01264	0.992	0.92	0.01660	0.990	0.84	0.02180	0.988
48	0.99	0.01029	0.997	0.93	0.01317	0.995	0.87	0.01679	0.993

3.4. Correlation between γ_r and t, σ_c

In this study, the relationship between γ_r and treatment time or confining stress has been studied. Figure 9(a) illustrates the correlation between the reference strain and the treatment time. In this study, the reference shear strain can be expressed by a power function of processing time.

$$\gamma_r = 1/(a + b \cdot t^c) \quad (5)$$

where t is the treatment time, a, b, and c are the fitting parameters. The fitting parameters a and b gradually decrease from 3503.8 to 2396.9 and 383.9 to 106.2 respectively and c increases from 0.74 to 0.92 with the confining stress increase from 25 kPa to 100 kPa.

Figure 9(b) shows the correlation between the reference shear strain and the confining stress. The γ_r increases with the increase of σ_c, and the difference of γ_r between different treatment times increase with the increase of σ_c. This also reflects that the confining stress still has a significant influence on the shear modulus attenuation curve of the sand sample with a lower cementation level. In addition, as shown in Figure 9(b), the difference of γ_r under different confining stress gradually decreases with the increasing treatment time, indicating that the effect of σ_c on the attenuation of shear modulus decreases during the treatment process. The relationship between γ_r and σ_c is linear and can be expressed by Eq.6 and the fitting *R-square* is greater than 0.99 in all cases.

$$\gamma_r = \delta \cdot \sigma_c + \phi \quad (6)$$

where δ, ϕ are the fitting parameters. As the treatment time increases, both δ and ϕ gradually decrease, which means the slope and intercept of γ_r - σ_c decrease.

Preprints (www.preprints.org) | NOT PEER-REVIEWED | Posted: 25 July 2022 doi:10.20944/preprints202207.0352.v1

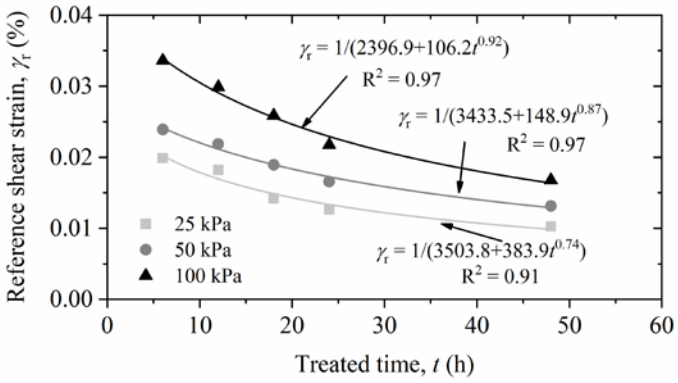

(a)

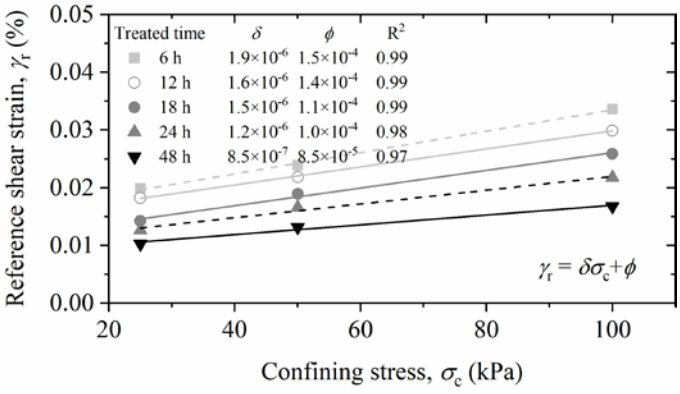

(b)

Figure 9. Variation in the reference shear strain with (a) treatment time, and (b) effective confining stress.

3.5. The damping ratio of MICP-treated calcareous sands

The results of the damping ratio curve are usually needed in the dynamic analysis procedures. The variation of damping ratio with strain amplitude (D-logγ relationship) is presented in Figure 10. The confining stress has a great impact on the response of damping ratio in the treated sample, that is a lower value at higher confining stress because of more interparticle contacts, therefore, less energy will be dissipated for the wave to propagate through.

As shown in Figure 11, it is observed that the damping ratio increases slightly when the shear strain amplitudes are smaller than 1×10^{-3}%, and once the shear strain amplitude exceeds 1×10^{-3} %, the damping ratio increases significantly with the increasing shear strain. It should be noted that the damping ratio firstly increases with the treatment time (6 hour-24 hours) and gradually decreases after being treated for about 24 hours. Some scholars had found similar results in the studies of treated soils [41,46]. Delfosse-ribay et al. [47] evaluated the damping ratio and shear modulus of the sand samples grouted by three different cementitious materials and found that the samples with higher dynamic shear modulus also have higher damping ratios. K. Saxena et al. [38] conducted some resonant column tests to study the dynamic moduli and damping ratios of cemented sands at low strains, they found that the damping ratio of cemented sands with a low level of cementation increases with the increases of cement content and reaches its maximum value at the cement content was about 5%~8% (defined as threshold cement content), and then it should decrease with further increase in cement content. In this study, the threshold calcium carbonate content is about 7% when the treatment time is about 24 hours.

Preprints (www.preprints.org) | NOT PEER-REVIEWED | Posted: 25 July 2022 doi:10.20944/preprints202207.0352.v1

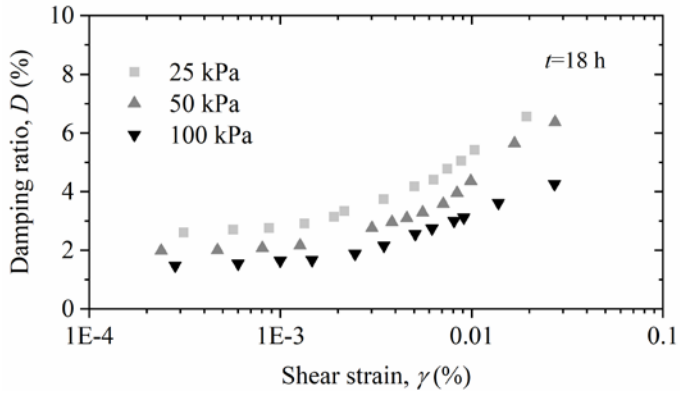

Figure 10. Damping ratio of samples treated for 18 hours under different confining pressure.

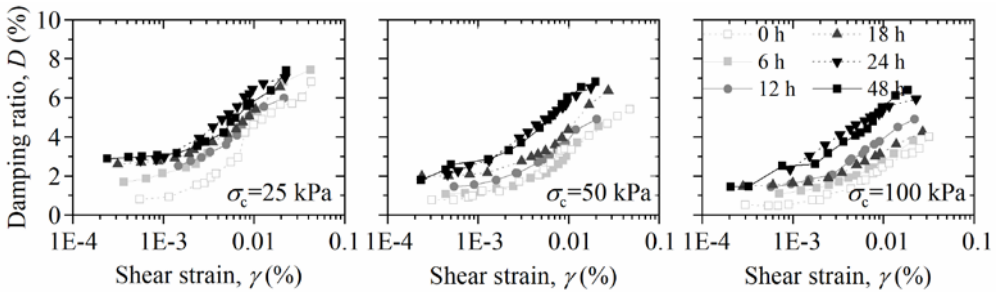

Figure 11. Comparison of damping ratio curves of calcareous sandy specimens with different treatment time.

4. Conclusions

In this study, a series of resonant column tests and unconfined compressive tests were conducted to evaluate the static strength and dynamic characteristics of MICP-treated calcareous sand. The study investigated the effect of the treatment time and confining stress on the shear modulus degradation and damping ratio. The relation between unconfined compressive strength and initial shear modulus were analyzed. Furthermore, the correlation between relative shear strain and treatment time, and confining stress was discussed. The conclusion can be expressed as follows:

1. After MICP treatment, the initial dynamic shear modulus and unconfined compressive strength were significantly increased, which indicates that the dynamic properties and strength of the calcareous sand are improved by the MICP treatment. The treated calcareous sandy sample shows higher strain sensitivity (strain-dependent) than that of untreated sands, and the strain sensitivity increases with the increasing of treated time, which indicates that the brittleness of MICP-treated calcareous sands is increased during treatment. The Hardin-Drnevich model can describe the G/G_0 attenuation law of MICP-treated calcareous sand. The shear modulus of the MICP-treated sand eventually approaches that of the untreated calcareous sand when the shear strain is approximately 0.03%.

2. The difference between the shear modulus of treated sand and that of untreated sand becomes more obvious as the confining stress increases because of the reduction of the pore volume of samples and the increase the contact between the particles. MICP cemented calcareous sand shows a significant improvement in the initial dynamic shear modulus G_0. The relationship between G_0 and confining pressure σ_c, as well as that between G_0 and unconfined compressive strength q_u, can be approximately described by a power function.

3. The difference of reference shear strain γ_r under different confining pressures gradually decreases with increasing treatment time, indicating that the influence of confining pressure on the attenuation curve of the dynamic shear modulus of MICP treated calcareous sand gradually decreases during the treatment process. The relationship between γ_r, t, and σ_c can be described by power function $\gamma_r = 1/(a + b \cdot t^c)$ and linear function $\gamma_r = \alpha \cdot \sigma_c + \beta$, respectively. The confining stress has a great impact on the response of the damping ratio in the treated sample. The threshold calcium carbonate content is about 7%.

Author Contributions: Conceptualization, Xinlei Zhang and Yumin Chen; methodology, Xinlei Zhang and Hongmei Gao; validation, Jun Guo and Ruibo Yi; formal analysis, Yi Han and Yumin Chen; investigation, Jun Guo; resources, Hanlong Liu and Hongmei Gao; data curation, Jun Guo and Ruibo Yi; writing—original draft preparation, Xinlei Zhang, Zhifu Shen; writing—review and editing, Lu Liu; visualization, Jun Guo.

Funding: This research was funded by National Natural Science Foundation of China, grant number 52179101, 52108324 and 52008207, Natural Science Foundation of Jiangsu for Young Researcher, grant number BK20190667, Natural Science Research Project of Colleges and Universities in Jiangsu Province of China, grant number 19KJB560015, and Postgraduate Research and Practice Innovation Program of Jiangsu Province, grant number KYCX22_1354.

Institutional Review Board Statement: Not applicable.

Informed Consent Statement: Not applicable.

Data Availability Statement: Not applicable.

Conflicts of Interest: The authors declare no conflict of interest.

References

1. Xiao, P.; Liu, H.L.; Xiao, Y.; Stuedlein, A.W.; Evans, T.M. Liquefaction resistance of bio-cemented calcareous sand. Soil Dyn Earthq Eng 2018, 107, 9–19.
2. Giretti, D.; Fioravante, V.; Been, K.; Dickenson, S.; Mesri, G.; Kane, T. Mechanical properties of a carbonate sand from a dredged hydraulic fill. Geotechnique 2020, 70, 937–42.
3. Sasanakul, I.; Gassman, S.; Ruttithivaphanich, P.; Dejphumee, S. Characterization of shear wave velocity profiles for South Carolina Coastal Plain. AIMS Geosci 2019, 5, 303–24.
4. Sharma, S.S.; Ismail, M.A.; Monotonic and Cyclic Behavior of Two Calcareous Soils of Different Origins. J of Geotech Geoenvironmental Eng 2006, 132, 1581–91.
5. Javdanian, H.; Jafarian, Y.; Dynamic shear stiffness and damping ratio of marine calcareous and siliceous sands Geo Marine Letters 2018, 315–22.
6. Shahnazari, H.; Rezvani, R. Effective parameters for the particle breakage of calcareous sands: An experimental study. Eng Geol 2013, 159, 98–105.
7. Qin, Z.G.; Yuan, X.M.; Cao, Z.Z.; M, H.G. Applicability and quality evaluation of foundation treatment method for backfilled coral sand site. Journal of Natural Disasters 2021, 1, 78-88, 2021. (in Chinese).
8. Xiao, Y.; Zhang, Z.; Stuedlein, A.W.; Evans, T.M. Liquefaction Modeling for Biocemented Calcareous Sand. J Geotech Geoenvironmental Eng 2021, 147, 04021149.
9. Xiao, Y.; Wang, Y.; Wang, S.; Evans, T.M.; Stuedlein, A.W.; Chu, J; Zhan, C.; Wu, H.R.; Liu, H.L. Homogeneity and mechanical behaviors of sands improved by a temperature-controlled one-phase MICP method. Acta Geotech 2021, 4.
10. Cheng, L.; Shahin, M.A.; Mujah, D; Influence of key environmental conditions on microbially induced cementation for soil stabilization. J Geotech Geoenvironmental Eng 2017, 143, 1–11.
11. Whiffin, V.S.; van Paassen, L.A.; Harkes. M.P. Microbial carbonate precipitation as a soil improvement technique. Geomicrobiol J 2007, 24, 417–23.
12. DeJong, J.T.; Fritzges, M.B.; Nüsslein, K. Microbially Induced Cementation to Control Sand Response to Undrained Shear. J Geotech Geoenvironmental Eng 2006,132, 1381–92.
13. O'Brien, P.L.; DeSutter, T.M.; Ritter, S.S.; Casey, F.X.M; Wick, A.F.; Khan, E.; Matthees, H.L. A large-scale soil-mixing process for reclamation of heavily disturbed soils. Ecol Eng 2017, 109, 84–91.
14. DeJong, J.T.; Mortensen, B.M.; Martinez, B.C.; Nelson, D.C. Bio-mediated soil improvement. Ecol Eng 2010, 36, 197–210.
15. Feng, K.; Montoya, B.M. Influence of confinement and cementation level on the behavior of microbial-induced calcite precipitated Sands under monotonic drained loading. J Geotech Geoenvironmental Eng 2015, 2, 04015057.

16. Minto, J.M.; Lunn, R.J.; El. Mountassir. G. Development of a Reactive Transport Model for Field-Scale Simulation of Microbially Induced Carbonate Precipitation. Water Resour Res 2019, 55, 7229–45.
17. Jonkers, H.M.; Thijssen, A.; Muyzer, G.; Copuroglu, O.; Schlangen, E. Application of bacteria as self-healing agent for the development of sustainable concrete. Ecol Eng 2010, 36, 230–5.
18. Wang, Z.; Zhang, N.; Jin, Y.; Li, Q.; Xu, J. Application of microbially induced calcium carbonate precipitation (MICP) in sand embankments for scouring/erosion control. Mar Georesources Geotechnol 2021, 39, 1459–71.
19. Zhang, X.; Chen, Y.; Liu, H.; Zhang, Z.; Ding, X. Performance evaluation of a MICP-treated calcareous sandy foundation using shake table tests. Soil Dyn Earthq Eng 2020, 129, 105959.
20. Fioravante, V.; Giretti, D.; Jamiolkowski, M. Small strain stiffness of carbonate Kenya Sand. Eng Geol 2013, 161, 65–80.
21. Giang, P.H.H.; Van. Impe, P.O.; Van. Impe, W.F.; Menge, P.; Haegeman, W. Small-strain shear modulus of calcareous sand and its dependence on particle characteristics and gradation. Soil Dyn Earthq Eng 2017, 100, 371–9.
22. Jafarian, Y.; Javdanian, H.; Haddad, A. Dynamic properties of calcareous and siliceous sands under isotropic and anisotropic stress conditions. Soils Found 2018, 58, 172–84.
23. He, H.; Li, W.; Senetakis, K. Small strain dynamic behavior of two types of carbonate sands. Soils Found 2019, 59, 571–85.
24. Shi, J.; Haegeman, W.; Cnudde, V. Anisotropic small-strain stiffness of calcareous sand affected by sample preparation, particle characteristic and gradation. Geotechnique 2021, 71, 305–19.
25. Shi, J.; Haegeman, W.; Xu, T. Effect of non-plastic fines on the anisotropic small strain stiffness of a calcareous sand. Soil Dyn Earthq Eng 2020, 139, 106381.
26. Morsy, A.M.; Salem, M.A.; Elmamlouk, H.H. Evaluation of dynamic properties of calcareous sands in Egypt at small and medium shear strain ranges. Soil Dyn Earthq Eng 2019, 116, 692–708.
27. Javdanian, H.; Jafarian, Y. Dynamic shear stiffness and damping ratio of marine calcareous and siliceous sands. Geo-Marine Lett 2018, 38, 315–22.
28. Hassanlourad. M.; Salehzadeh. H.; Shahnazari. H. Dilation and particle breakage effects on the shear strength of calcareous sands based on energy aspects. Int J Civ Eng 2008, 6, 108–19.
29. Khalil, A.; Khan, Z.H.; Attom, M.; EI Emam, M.; Fattah, K. Dynamic Properties of Calcareous Sands from Urban Areas of Abu Dhabi. Applied Sciences, 2022, 12(7): 3325.
30. Liang, K.; He, Y.; Chen, G.X. Experimental study of dynamic shear modulus and damping ratio characteristics of coral sand from Nansha Islands. Rock and Soil Mechanics 2020, 1, 23-38. (in Chinese).
31. Jafarian. Y.; Javdanian. H. Small-strain dynamic properties of siliceous-carbonate sand under stress anisotropy. Soil Dyn Earthq Eng 2020,131, 106045.
32. Shi, J.; Xiao, Y.; Hu, J; Wu, H.; Liu, H. Haegeman W. Small-Strain Shear Modulus of Calcareous Sand under Anisotropic Consolidation. Can Geotech J 2021.
33. Lang, L.; Li, F.; Chen. B. Small-strain dynamic properties of silty clay stabilized by cement and fly ash. Constr Build Mater 2020, 237, 117646.
34. Subramaniam, P.; Banerjee, S.; Ku, T. Shear Modulus and Damping Ratio Model for Cement Treated Clay. Int J Geomech 2019, 19, 06019010.
35. Feng, K.; Montoya, B.M. Drained Shear Strength of MICP Sand at Varying Cementation Levels. Ifcee 2015, 2242–51.
36. Simatupang, M.; Okamura, M.; Hayashi, K.; Yasuhara, H. Small-strain shear modulus and liquefaction resistance of sand with carbonate precipitation. Soil Dyn Earthq Eng 2018, 115, 710–8.
37. Acar, Y.B.; El-Tahir, E.T.A. Low strain dynamic properties of artificially cemented sand. J Geotech Eng 1986, 112, 1001–15.
38. Saxena, S.K.; Avramidis, A.S.; Reddy, K.R. Dynamic moduli and damping ratios for cemented sands at low strains. Can Geotech J 1988, 25, 353–68.
39. Lin, B.; Zhang, F.; Feng, D.C.; Tang, K.W.; Feng, X. Dynamic shear modulus and damping ratio of thawed saturated clay under long-term cyclic loading. Cold Reg Sci Technol 2018, 145, 93–105.
40. Gao, H.M.; Xia, S.S.; Chen, F.Y.; Stuedlein, A.W.; Li, X.; Wang, Z.H.; Shen, Z.F.; Chen, Y.M. Dynamic shear modulus and damping of cemented and uncemented lightweight expanded clay aggregate (LECA) at low strains. Soil Dyn Earthq Eng 2021, 142, 106555.
41. Hardin, B. O.; Drnevich, V.P. Shear modulus and damping in soils: design equations and curves. J Soil Mech Found Div 1972, 98, 667–92.
42. Consoli, N.C.; Viana, Da.; Fonseca, A.; Cruz, R.C.; Heineck, K.S. Fundamental Parameters for the Stiffness and Strength Control of Artificially Cemented Sand. J Geotech Geoenvironmental Eng 2009, 135, 1347–53.
43. Porcino, D.; Ghionna, V.N.; Granata, R.; Marcianò, V. Laboratory determination of mechanical and hydraulic properties of chemically grouted sands. Geomech Geoengin 2016, 11, 164–75.
44. Liu, Q.F.; Zhuang, H.Y.; Wu, Q.; Zhao, K.; Chen, G.X. Experimental study on dynamic modulus and damping ratio of rubber-sand mixtures over a wide strain range. J Earthq and Tsunami, 2022, 16(02), 2140006.
45. Hardin, B.O.; Drnevich, V.P. Shear modulus and damping in soils: measurement and parameter effects. J Soil Mech Found Div 1972, 98, 603–24.
46. Wang, Z.Y.; Mei, G.X.; Yu, X.B. Dynamic Shear modulus and damping ratio of waste granular rubber and cement soil mixtures. Adv Mater Res 2011, 243, 2091–4.

 doi:10.20944/preprints202207.0352.v1

47. Delfosse-ribay, E.; Djeran-maigre, I.; Cabrillac, R.; Gouvenot, D. Shear modulus and damping ratio of grouted sand. Soil Dyn Earthq Eng 2004, 24, 461–71.